Pesticide Biochemistry and Physiology 205 (2024) 106127

Contents lists available at ScienceDirect

Pesticide Biochemistry and Physiology

journal homepage: www.elsevier.com/locate/pest

Fatty acid synthase 2 knockdown alters the energy allocation strategy between immunity and reproduction during infection by *Micrococcus luteus* in *Locusta migratoria*

Tingting Ma [1], Ya Tang [1], Yi Jin, Jiaying Xu, Huazhang Zhao, Min Zhou, Bin Tang, Shigui Wang [*]

Hangzhou Key Laboratory of Animal Adaptation and Evolution, College of Life and Environmental Sciences, Hangzhou Normal University, Hangzhou, Zhejiang 311121, China

ARTICLE INFO

Keywords:
Fatty acid synthase 2
Energy
Immunity
Reproduction
Locusta migratoria

ABSTRACT

Immunity and reproduction are vital functions for the survival and population maintenance of female insects. However, owing to limited resources, these two functions cannot be fulfilled simultaneously, resulting in an energy tradeoff between them. Notably, the mechanisms underlying this immune-reproductive trade-off, in which energy competition likely plays a central role, remain poorly understood. Fatty acid synthase (*FAS*), a key gene involved in lipid synthesis and insect energy metabolism, was investigated in this study using *Locusta migratoria* as the research subject. Bacterial infection and RNA interference (RNAi) technology were used to examine changes in the immunity, fecundity, and energy metabolism patterns of locusts under different treatments. The findings of this study demonstrate that infection with *Micrococcus luteus* triggers an immune response in locusts, significantly upregulates the expression of defensin 3 (*DEF3*) and *Attacin*, and enhances pHenoloxidase (PO) activity. Upon *FAS2* silencing, bacterial attack upregulated *DEF3* and *Attacin* expression to a lesser extent, leading to increased lysozyme activity instead of PO. Furthermore, bacterial infection results in a decrease in glycogen and glucose content in the fat body, accompanied by a significant increase in triacylglycerol (TAG) content. However, after *FAS2* knockdown, both the lipid and carbohydrate contents were significantly reduced in the fat body. Compared with bacterial infection alone, low *FAS2* expression further exacerbated fecundity impairment in locusts. The expression levels of vitellogenin A (*VgA*) and vitellogenin B (*VgB*) were significantly low, with severe ovarian atrophy observed. Notably, the ovarian weight was only 21 % compared to that of the control group. Moreover, females exhibited minimal egg-laying behavior. In summary, our findings suggest that following *FAS2* gene silencing, there is a greater inclination toward immune stimulation energy activation in locusts, whereas reproductive investment is reduced. The outcomes of this study will contribute to the further exploration of the molecular mechanisms underlying the trade-off between immune and reproductive energy in locusts.

1. Introduction

Insects lack the acquired immune response observed in mammals and rely primarily on a robust innate immune system, encompassing both cellular and humoral immunity, to combat foreign pathogen invasion. Upon pathogen invasion, insects use cellular immune responses mediated by blood cells (plasma cells and granulocytes), including phagocytosis, nodule formation, and pathogen encapsulation (Zhang et al., 2021). In addition, insects exhibit humoral immune reactions involving the production of antimicrobial peptides (AMPs), lectins, reactive oxygen species, and other immune effectors, such as lysozyme and phenoloxidase (PO) cascade reactions, for defense purposes (Cerenius et al., 2008; Levitin and Whiteway, 2008; Jiang et al., 2010). The Toll and Imd pathways play pivotal roles in protecting insects

* Corresponding author.
E-mail addresses: 2022111010007@stu.hznu.edu.cn (T. Ma), tangya678678@163.com (Y. Tang), 2022210301227@stu.hznu.edu.cn (Y. Jin), 2023111010043@stu.hznu.edu.cn (J. Xu), zhaohuazhang163@outlook.com (H. Zhao), tbzm611@126.com (M. Zhou), tbzm611@hznu.edu.cn (B. Tang), sgwang@hznu.edu.cn (S. Wang).
[1] These authors contributed equally to this study.

https://doi.org/10.1016/j.pestbp.2024.106127
Received 9 July 2024; Received in revised form 7 September 2024; Accepted 8 September 2024
Available online 12 September 2024

against bacterial and fungal infections. In response to fungal and most gram-positive bacterial infections, insects primarily induce antimicrobial peptide expression through activation of the Toll pathway. Conversely, in response to gram-negative bacterial infections, AMPs primarily induce antimicrobial peptide expression via the Imd pathway activation (Hillyer, 2016).

The synthesis of vitellogenin (Vg) and its selective uptake by developing oocytes is a pivotal event in female insect reproduction, representing a significant milestone (Wu et al., 2021). Vg was initially identified in the hemolymph of *Hyalophora cecropia* (Telfer, 1954). Subsequent studies confirmed that Vg is synthesized in the fat body of most insects and is subsequently secreted into the hemolymph. Vg is taken up, deposited, and converted into vitellogenin by oocytes through endocytosis, which is mediated by the vitellogenin receptor (VgR), to provide essential nutrients and energy for oocyte maturation and embryonic development (Roth and Porter, 1964; Han et al., 2022). VgR plays a crucial role in facilitating the uptake of Vg by oocytes, with low expression levels leading to the retardation of ovarian development and a significant reduction in egg production (Cong et al., 2015; Ma et al., 2018). Therefore, the substantial synthesis and uptake of Vg are indispensable for insect vitellogenesis, egg maturation, and ovarian development.

Both immune defense and reproductive processes are energetically costly and require substantial resource inputs. Because of the limited availability of resources, it is not feasible to meet the demands of these two physiological processes simultaneously. In insects, there is a trade-off between various life history characteristics to achieve optimal resource allocation (Denno, 1994; Schwenke et al., 2016; Jehan et al., 2022). Particularly in multifunctional organs within an individual organism, when multiple processes rely concurrently on the same organ, the phenomenon of mutual constraints and resource trade-offs between each function becomes particularly evident. The adipose body of insects serves as a typical multifunctional organ in which numerous metabolic activities occur. It functions as a hub for energy metabolism and as the primary site for synthesizing Vg proteins and antimicrobial peptides involved in immunity (Arrese and Soulages, 2010; Hillyer, 2016; Toprak et al., 2020; Gupta et al., 2022). This trade-off phenomenon has been observed in numerous female insects, wherein an increase in reproductive investment results in a concomitant decrease in immune function. Consequently, this compromised immunity leads to susceptibility to infections and the subsequent activation of the immune system, ultimately resulting in reduced reproductive output (Schwenke et al., 2016). During immune challenges, the activation of the immune response to enhance the resistance of the body to infection often entails a trade-off with allocated resources for other life history traits (Nystrand and Dowling, 2020). Activation of the immune system during a bacterial attack on *Apis mellifera* results in decreased levels of hemolymph storage proteins, including Vg proteins. This adaptive response reallocates resources toward combating infection within the body (Lourenco et al., 2009).

Lipids and carbohydrates are essential energy substrates for organismal growth and development. Fatty acid biosynthesis involves multiple enzymatic reactions, wherein acetyl-CoA carboxylase (ACC) catalyzes the conversion of acetyl-CoA into malonyl-CoA, a substrate used by fatty acid synthase (FAS) during fatty acid synthesis, resulting in the formation of long-chain fatty acids (Visser and Ellers, 2008). Triacylglycerol (TAG) constitutes >90 % of lipids present in adipose body (Canavoso et al., 2001). TAG content accounts for 30–40 % of egg dry weight—an essential component necessary for egg maturation and maintenance of normal life activities (Kawooya and Law, 1988; Heier and Kühnlein, 2018). Trehalose, a non-reducing disaccharide, is the predominant sugar in insect hemolymph and serves as the primary energy source, thus commonly referred to as “blood sugar” (Shukla et al., 2015). Trehalose synthesis is primarily regulated by two enzymes: trehalose-6-phosphate synthase (TPS) and trehalose 6-phosphate phosphatase (TPP). Trehalose can only be used after its conversion into glucose, and its degradation is solely controlled by trehalase (TRE) at present (Shukla et al., 2015; Wang et al., 2020a, 2020b). Glycogen synthesis and mobilization are governed by glycogen synthase (GS) and phosphorylase (GP), respectively (Friedman, 1978; Arrese and Soulages, 2010; Zeng et al., 2020). In insects, energy storage and use rely on the interconversion of glucose, trehalose, and glycogen (Hou et al., 2015).

Locusta migratoria is an important agricultural pest known for its high fertility, which contributes to outbreaks in locusts (Sangbaramou et al., 2018). Locust disasters belong to the violent locust plague category, and once a violent locust plague occurs, it can cause devastating disasters. RNA interference (RNAi) technology is a novel, green, and sustainable control strategy that has gained widespread application in crop pest management because of its high efficiency and specificity. The study showed that the selection for individuals sensitive to ds*CRZ* of the migratory locust *Locusta migratoria* produced a dramatic increase in the RNAi sensitivity in the following generations (Sugahara et al., 2017). RNAi refers to the targeted degradation of specific gene sequences triggered by endogenous or exogenous double-stranded RNA (dsRNA) molecules (King et al., 2020; Hough et al., 2022). Animal fatty acid synthase (FAS) is an essential multifunctional enzyme and a highly conserved key gene involved in fatty acid (Wang et al., 2020a, 2020b). The *FAS* gene has been extensively studied in various insects, including *Rhodnius prolixus*, *Blattella germanica*, *Helicoverpa armigera*, and *Colaphellus bowringi*, where it plays essential roles in lipid synthesis and reproductive processes (Alabaster et al., 2011; Li et al., 2016; Tan et al., 2017; Ma et al., 2018; Moriconi et al., 2019; Pei et al., 2019). In this study, bacterial infection combined with RNAi technology was used to investigate the impact of the *FAS2* gene on the immune response and reproductive energy allocation in locusts. Our findings provide potential targets for future biological pest control strategies.

2. Materials and methods

2.1. Insects and bacteria

L. migratoria eggs were procured from the Huaibei breeding farm in the Anhui Province and incubated in a controlled environment chamber. The incubation procedure was as follows: the eggs were placed in a box (10 × 15 × 20 cm) containing moist sand at the bottom with a depth of 2–3 cm and were reared at 30 ± 2 °C and 80 % RH, with a 16 h: 8 h (L:D) photoperiod. The eggs were covered with vermiculite to maintain optimal humidity. After hatching, the locusts were transferred to well-ventilated cages (50 × 50 × 50 cm) at 150–200 locusts per cage and provided fresh wheat and wheat bran as their diet.

The strain of *M. luteus* was obtained from Beijing Biobw Biological Company (Beijing, China) and activated before the experiment. *M. luteus* was cultured in liquid medium at 37 °C and 250 rpm/min in a constant temperature oscillator (Suzhou Peiying, China). Liquid medium (100 mL): Glucose (Sangon Biotech, China) 0.25 g, peptone (Sangon Biotech, China) 1.7 g, sodium chloride (Sangon Biotech, China) 0.5 g, dipotassium hydrogen phosphate (Sangon Biotech, China) 0.25 g, distilled water supplemented to 100 mL. The strain was cultured to an 600_{nm} of 0.9. The bacterial suspension was centrifuged at 5000 rpm for 5 min to remove the culture medium, followed by washing thrice with sterile phosphate-buffered saline (PBS). Finally, the suspension was stored in a refrigerator at 4 °C for subsequent use.

2.2. Bacterial infection and injection of dsFAS2

Injection of bacteria alone. After day 4 post-adult emergent (PAE), *M. luteus* was injected into the abdominal cavity to induce an immune response (10 μL/ head), and an equal amount of PBS was injected as a control.

Combined injection of bacteria and dsRNA. The full-length sequence of *FAS2* was obtained from the *L. migratoria* genome database, and specific primers used for *FAS2* polymerase chain reaction (PCR)

amplification and dsRNA synthesis were designed using Primer 5.0 software (Table 1). Green fluorescent protein (*GFP*) gene was used as the negative control. dsFAS2 (482 bp) and dsGFP (365 bp) were synthesized in vitro using the T7RiboMAX Express RNAi System (Promega Corporation, WI, USA). The female locusts were injected with 20 μg/ head of dsRNA at the early eclosion stage. Bacterial infection was conducted in a manner similar to that described above, with the injection taking place 4 d later.

2.3. Sample collection and data collection

Tissue sampling. Hemolymph, adipose bodies, and ovarian tissues from both experimental and control groups were collected 24 h after injection. The samples were snap-frozen in liquid nitrogen and stored in a refrigerator at −80 °C, and the hemolymph was stored at −20° for subsequent experiments. Three biological replicates consisting of at least five specimens were established for each sample.

Survival analysis. For the survival analysis of locusts treated with *M. luteus*, 30 insects were injected with *M. luteus* on day 4 PAE. Mortality was recorded every 24 h for seven d. The number of days from injection to death was documented, and each treatment group had three biological replicates consisting of at least eight samples. In the experimental group that received combined injections of bacteria and dsRNA, the number of days from the injection of *M. luteus* to the death of the female worms was recorded. Each treatment consisted of three biological replicates, each containing at least eight specimens.

Morphological observations of fat bodies and ovaries. To investigate the effect of bacterial infection or *FAS2* silencing on fat accumulation and ovarian development in locusts, we used a camera (Canon, Tokyo, Japan) to capture images of fat body morphology. The morphology of the ovarian samples was photographed using a dissecting stereomicroscope (Leica, Germany). In the experimental group injected *M. luteus* alone, locusts at day 4 PAE were injected with *M. luteus*. After 24 h, the fat body and ovaries were carefully dissected and photographed, and the weight of each ovary was recorded. A minimum of 15 locusts was dissected from each group. In the experimental group with the combined injection of bacteria and dsRNA, locusts within day 0 PAE received ds*FAS2* injection followed by *M. luteus* injection after 4 d. After an additional 24 h, both fat bodies and ovaries were dissected for photography while recording the weight of each ovary. A minimum of 15 locust samples were dissected from this group.

Fecundity analysis. To investigate the effect of bacterial infection or *FAS2* silencing on locust fertility, various reproductive indices of female locusts were recorded, including the pre-oviposition period, egg count, and number and weight of egg pods. In the group treated with *M. luteus* alone, locusts were injected with *M. luteus* on day 4 PAE and the time from day 0 to the first egg laying during early oviposition was recorded. Other parameters such as the average number of eggs laid and the number and weight of egg pods within 11 d after bacterial injection were also documented. In the experimental group with the combined injection of bacteria and dsRNA, locusts were injected with ds*FAS2* on day 0 PAE, followed by *M. luteus* injection after 4 d. The fecundity indices of the treatment groups were consistent. Each treatment included three biological replicates consisting of no more than five specimens.

2.4. RNA extraction and reverse transcription-quantitative polymerase chain reaction (RT-qPCR)

Total RNA was extracted using the TRIzol reagent (Invitrogen, USA) in accordance with the manufacturer's instructions. The concentration and purity of total RNA were measured using a NanoDrop 2000 spectrophotometer (Thermo Scientific, America) and 1.0 % agarose gel electrophoresis, respectively. For reverse transcription, the first strand of cDNA was synthesized using a PrimeScriptTM RT Reagent Kit (Takara, Japan). The cDNA of each sample was diluted tenfold and used as an RT-qPCR template on the Bio-Rad Real-Time PCR Assay System (Bio-Rad, USA), using Premix Ex Taq (SYBR Green) reagents from Takara. The reaction program initiated at 95 °C for 3 min, followed by 40 cycles consisting of denaturation at 95 °C for 10 s, annealing at 58 °C for 15 s, and extension at 72 °C for 20 s. *β-actin* served as an internal reference gene, and relative gene expression levels were calculated using the $2^{-\Delta\Delta Ct}$ method. The RT-qPCR primers used Primer 5.0 software (Table 1), with each sample having three biological replicates comprising no fewer than five test worms.

Table 1
Primers used for PCR.

Primer name	F-Primer sequence (5′–3′)	R-Primer sequence (5′–3′)	
GFP	AAGGGCGAGGAGCTGTTCACCG	CAGCAGGACCATGTGATCGCGC	cDNA clones
FAS2	ACGGAACAGGCACTAAA	GAACCAGGCTGATAAAG	
ACC	GTGTGTTGGAGCCAGAAGGAAT	CACTTGGAAGGTTAGGAGAGGA	
Attacin	GTGCTCCTCGTCGTTCTGA	CCCACGCCTTTCTCTCTGT	
β-actin	GACGAAGAAGTTGCCGCTC	TCCCATTCCCACCATCACA	
Bmm	ATCACTGACGAGGGTCTACGA	ATACTGGTGTTGGCGAGGTT	
Cactus	ATCCAAATGGCACCTCACC	CTGCGACTACAAGCCTTCTAACT	
DEF3	AGGGCTACAAGGGAGGACAC	CATCAGCAGGCAAGAAACAAG	
DEF4	GAAACCTCGTGCGAGCAGA	CGATGCCAGCAGTGGTAAGG	
ELO6	CTGCAATGACTCTGGTCCGATAA	GCGCTGGTCACTCCTGTTGTC	
FAR	CACGGCGTACTGTCACTTG	TCAGCACTGGTAAACCCTTC	
FAS2	TTAGTGGAAAGGGAGGC	CCATACAAGGGTCAGGT	
GNBP1	TTTTCCCCGAGATTTGGC	TTGCTATTCTTATCTGCCCTGAC	
GS	ACTCCGAATGGTCTCAATGTCA	GGTAGGGAATATCAGGAATGCA	
GP	CCCTGGTGACCTAGACAAACT	GGGTGTCATCTCATAGAAATCG	RT-qPCR
Lip3	GGTCGGATTTGATGCC	TGAGCCAGGGTCTTTGTA	
Lsd-1	TGTCACTTGGAGGAGAAAA	AAGGTCGGAGTATCAGCAC	
Lsd-2	GCTCCGAAAATGGAATGC	TGCCTCAGCCGTTGATAGT	
MyD88	CAGAAACATCGGAAAGTGGTA	TCGTATGGTGCTGAATGGTAT	
Spaetzle	TCAAAGTGGCAGTGGTTCTCA	CACAAGCTGGGTGTAACGATC	
Pelle	TCCTCAACCATCTGCTCCTT	CATTTCGTTCACTGCTTATCAC	
TPS	AGACGAACGGACACTACGAATGA	ATCCTCCCTTAGCGAACCCATC	
TRE	GCACTCCATAATCAAGCAGCAC	TAATGAACCATCGCCCAGAG	
VgA	CTCTTTCGTCCAACAGCCG	CTCGCAACCATTCCCTTCA	
VgB	GGCAGTTTTGCTTATTATGGG	TTCCGGGTTTGACAGTTGG	
VgR1	ATAAAGGTCTACCATCCAGCCC	GACAGGCACAGGTGTAGGAGTT	
VgR2	GGCAAAAGGGATCACTCGA	GCCACCATCAGCCCAAAAT	
dsGFP	TAATACGACTCACTATAGGGAGAAAGGGCGAGGAGCTGTTCACCG	TAATACGACTCACTATAGGGAGACAGCAGGACCATGTGATCGCGC	dsRNA synthesis
dsFAS2	TAATACGACTCACTATAGGGAGAACGGAACAGGCACTAAA	TAATACGACTCACTATAGGGAGAGAACCAGGCTGATAAAG	

2.5. Enzyme activity determination

The activities of phenoloxidase and lysozyme were determined following previously established methods with appropriate modifications (Tang et al., 2023). Specifically, enzyme activity was detected using the hemolymph supernatant. Protein concentrations were measured using a BCA protein Assay Kit (Takara, Japan) with bovine serum albumin (BSA) as the standard.

Determination of PO activity: 60 μL serum diluent was added to 240 μL phosphate-buffered saline (PBS) (pH 6.4) buffer and 360 μL L-3, 4-dihydroxyphenylalanine (L-dopa) (3 g/L). The 200 μL mixture was added to the microplate, and the absorbance A0 was measured at 490 nm using Thermo Fisher Scientific (America). Following incubation at 37 °C for 30 min, the absorbance A at 490 nm was recorded, and PO activity was quantified as ΔA490 /mg protein.

Lysozyme was measured using a lysozyme test kit from Nanjing Jiancheng in accordance with the instructions provided by the manufacturer. The activity of lysozyme was quantified as ΔA530 /mg protein.

2.6. Determination of glycogen, trehalose and glucose content

The hemolymph supernatant collected from the samples was directly used to quantify the levels of glycogen, trehalose, and glucose. To determine the contents of these substances in the fat body, the weight (g): volume (mL) = 1:10 was maintained by adding PBS to the fat body. The mixture was thoroughly ground using a grinder and ultrasonicated to ensure complete cell disruption. The resulting homogenate was then centrifuged at 2500 rpm at 4 °C for 20 min, and the resulting supernatant was used to measure glycogen, trehalose, and glucose concentrations. Each treatment included three biological replicates, with no fewer than five specimens.

The glycogen content was determined following the method described by Mollaei et al. (2017), with appropriate modifications. Briefly, 30 μL of hemolymph or fat body supernatant was mixed with 600 μL of anthrone solution (0.02 g anthraquinone (Sinopharm, China) dissolved in 10 mL of 98 % sulfuric acid) and reacted at 90 °C for 10 min. The light absorption at 620 nm was measured using a Thermo Fisher Scientific (USA), and the glycogen content was calculated based on a standard curve.

The trehalose and glucose levels were determined as described by Wang et al. (2020a, 2020b). The trehalose content was determined using the anthranone method. In the first step, 30 μL supernatant was mixed with an equal volume of 1 % sulfuric acid. The reaction conditions included incubation in a water bath at 90 °C for 10 min, followed by cooling at 0 °C for 3 min. In the second step, 30 μL of a 30 % potassium hydroxide (Sinopharm, China) solution was added to the previous reaction mixture under identical conditions as before. Lastly, in the third step, 600 μL of anthrone solution was added to the reaction mixture from the previous step and incubated under similar conditions as before. After completion of the reaction, the absorbance at 630 nm was measured using an enzyme marker to calculate the trehalose content based on a standard curve. The glucose content was measured using a Glucose (GO) Assay Kit (Sigma-Aldrich, USA).

2.7. Determination of TAG and free fatty acid (FFA) contents

According to the manufacturer's instructions, the levels of TAGs and FFAs in the hemolymph, ovary, and adipocytes were quantified using a TAG test kit (Nanjing Jiancheng, China) and a FFA content detection kit (Solarbio, China).

2.8. Detection of Vg by ELISA assay

The Vg content in the fat body, ovary, and hemolymph was quantified using an indirect double-antibody sandwich ELISA method based on the protocol of Guo et al. (2011) with appropriate modifications. For the hemolymph samples, the Vg content was determined from the supernatant collected after centrifugation. Tissue samples were mixed with PBS at a weight (g)-to-volume (mL) ratio of 1:10 and thoroughly homogenized using a grinder, followed by ultrasonication to ensure complete cell disruption. The resulting homogenate was then centrifuged at 8000 rpm for 10 min at 4 °C, and the obtained supernatant was used for Vg content analysis.

The specific steps are as follows: The supernatant was diluted with the coating solution (1.59 g Na_2CO_3 and 2.93 g $NaHCO_3$ dissolved in 1000 mL sterile water) at an appropriate ratio, thoroughly mixed, and 100 mL of the mixture was added to each well of a 96-well microplate (Sangon, China). After sealing the plate, it was incubated at 37 °C for 4 h and then fixed. The plate was then rinsed five times with phosphate-buffered saline with Tween (PBST; Sangon, China) for 1 min each time. To seal, 400 μL of a 5 % skim milk powder solution (Sangon, China) was added to each well, followed by sealing with a film cover, incubation at 37 °C for 2 h, and washing thereafter. For primary antibody incubation, 100 μL of Vg protein antibody diluted in PBST (ratio, 1:1000) was added to each well (GenScript, China), after which the plate was sealed with a membrane, incubated at 37 °C for 2 h, and washed again to remove unbound primary antibody. For incubation of the secondary antibody, 100 μL of enzyme-labeled goat anti-rabbit was added to each well (diluted in PBST; ratio, 1:5000) (biosharp, China), after which the plate was sealed with a membrane, incubated at 37 °C for 1 h, and washed again to remove unbound secondary antibody. For the color development reaction, 100 μL TMB color development solution was added to each well (Beyotime, China), and the plate was incubated at 37 °C for 10 min until the reaction is visible. Finally, 50 μL of 2 M H_2SO_4 was added to each well to stop the reaction, and the absorbance values were measured at 450 nm using enzyme labeling.

2.9. Data statistics and analysis

Kaplan-Meier survival analysis was used to assess changes in the locust survival rate. Except for adipose body and ovarian morphological development, all other data were subjected to Student's *t*-test using SPSS software (version 26.0) to determine significant differences between groups (* $P < 0.05$, ** $P < 0.01$, and *** $P < 0.001$). The data are presented as the mean ± standard error (SE) of three replicates.

3. Results

3.1. Immune response alterations and survival analysis of locusts after *M. luteus* infection

After infection with *M. luteus*, the expression of genes related to immune signaling pathways was analyzed. The results revealed a significant downregulation in the expression of *Spaetzle*, whereas *MyD88*, *Pelle*, and *Cactus* were upregulated without statistical significance (Fig. 1). However, infection with *M. luteus* induced a substantial increase in antimicrobial peptides expression. *DEF3* and *Attacin* exhibited 8.1 and 8.6-fold increases, respectively, compared to the control group (Fig. 1A). Furthermore, the injection of *M. luteus* resulted in elevated phenol oxidase activity but decreased lysozyme activity compared with the control group (Fig. 1B). Mortality data were recorded for 7 d, starting from the day of injection. Survival analysis demonstrated that locusts injected with PBS had an 80 % survival rate whereas those injected with *M. luteus* only had a survival rate of 36.7 % (Fig. 1C), leading to a significantly shortened adult lifespan by approximately 1.8 d (PBS = 11.5 vs *M. luteus* = 9.7) compared to the control group (Fig. 1D). These findings indicate that infection with *M. luteus* activates the immune response of locusts but also negatively affects their viability.

3.2. Influence of *M. luteus* infection on energy metabolism of locusts

To investigate the impact of *M. luteus* infection on energy metabolism

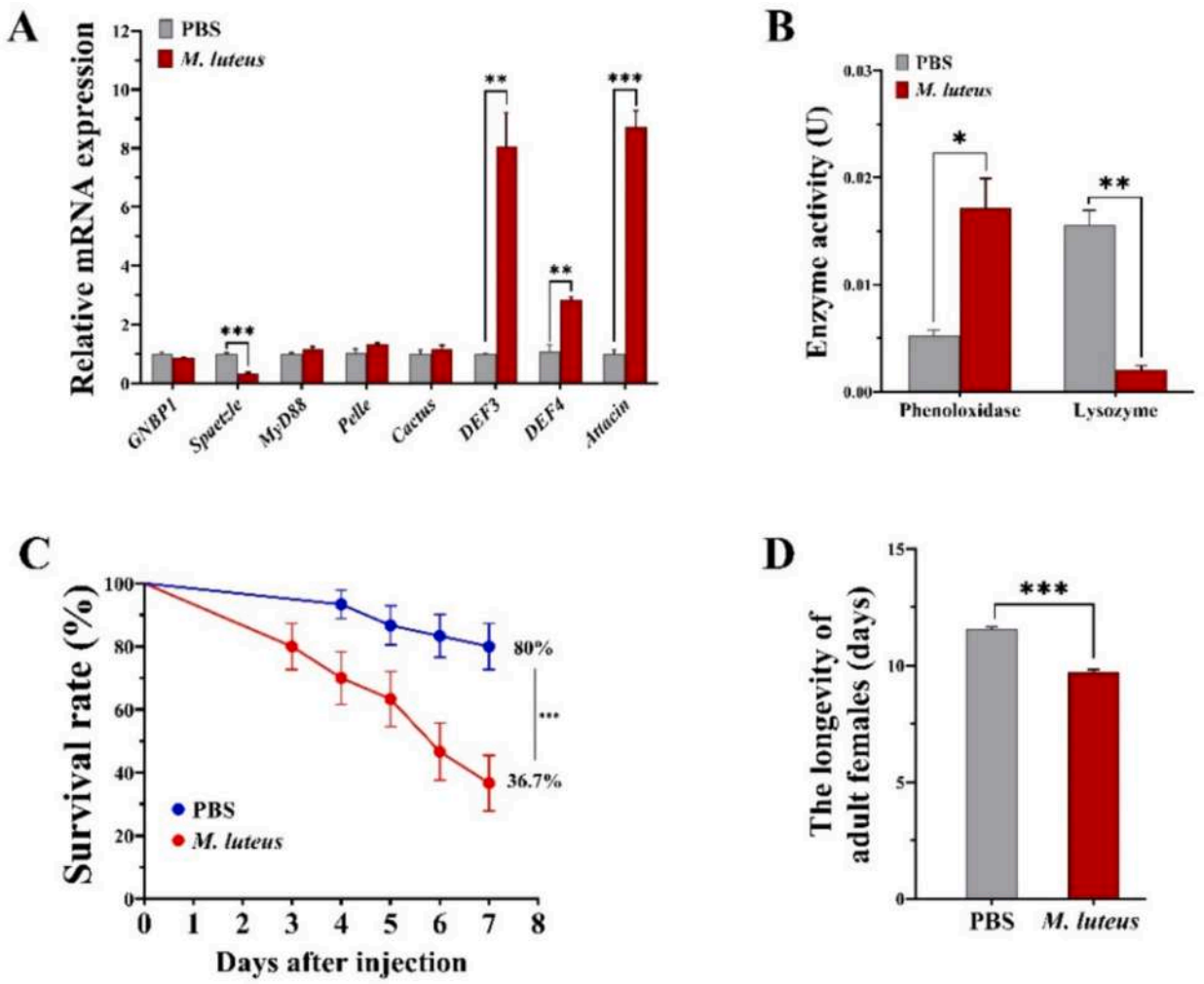

Fig. 1. Immune response alterations and survival analysis of locusts infected with *M. luteus*. (A) Expression levels of Toll immune pathway-related genes were quantified. (B) PO and lysozyme activities were measured. Each experimental group consisted of three biological replicates with a minimum of five locusts per replicate. (C) Changes in the survival rate of locusts were monitored after injection with *M. luteus*, and mortality was recorded every 24 h for 7 d. Each treatment group included 30 locusts, and Kaplan-Meier survival analysis was performed. (D) Time from emergence to adult death after injection of *M. luteus* was measured in days. Each experimental group consisted of three biological replicates with a minimum of eight locusts per replicate. Each value is presented as the mean ± SE, and statistically significant differences between the groups are denoted by * ($P < 0.05$), ** ($P < 0.01$), and *** ($P < 0.001$) using the Student's *t*-test.

in locusts, the expression levels of genes associated with carbohydrate and lipid metabolic pathways as well as the levels of related energy substances were examined 24 h after injecting *M. luteus*. In terms of carbohydrate and water metabolism, compared to the control group injected with PBS, the injection of *M. luteus* significantly upregulated *GP* expression and significantly reduced glucose content in both fat bodies and hemolymph. In addition, it led to a decrease in the glycogen content in the fat body (although not statistically significant). Trehalose content in fat body and hemolymph showed a significant increase compared to the control group, increasing by 142.4 % and 27.6 %, respectively (Figs. 2A and B). Interestingly, the injection of *M. luteus* appeared to promote lipid accumulation in locusts. Our findings indicated that infection with *M. luteus* significantly upregulated the expression of genes related to lipid metabolism, such as *FAS2*, *Lsd-2*, and *Lip3*, resulting in a significant increase in the TAG content within the adipose bodies (Figs. 2C and D). Furthermore, FFA content was notably higher than that observed in the control group for both fat bodies (increased by 89.6 %) and ovarian tissue (increased by 33.0 %) (Fig. 2E). Morphological observations revealed considerably greater abdominal cavity fat accumulation in the experimental group than that in the control group (Fig. 2F).

3.3. Influence of *M. luteus* infection on ovarian development of locusts

The effects of *M. luteus* infection on ovarian development were investigated by measuring the expression of *Vgs*, *VgRs*, and Vg in locusts. Changes in the ovarian weight and morphology were recorded. These results demonstrate that *M. luteus* infection significantly inhibits vitellogenin gene expression. First, compared to the control group, the expression of *VgA* and *VgB* in the fat body was markedly downregulated, with reductions of 77.6 % and 73.7 %, respectively (Fig. 3A). Furthermore, there was a significant decrease in hemolymph (72.8 %) and ovary Vg protein content (57.7 %) in the experimental group than that observed in the control group (Fig. 3B). Morphological observations revealed that injection of *M. luteus* resulted in significantly reduced volume of the ovary and primary oocyte, as well as decreased length of the ovarian duct. Ovary weight was notably lower than that in the control group (Figs. 3C and D). These findings indicate that *M. luteus* infection inhibits ovarian development in locusts.

3.4. Influence of *M. luteus* infection on fecundity of locusts

The injection of *M. luteus* resulted in a significant extension of the ovulation period in locusts, with a duration approximately 0.9 d longer

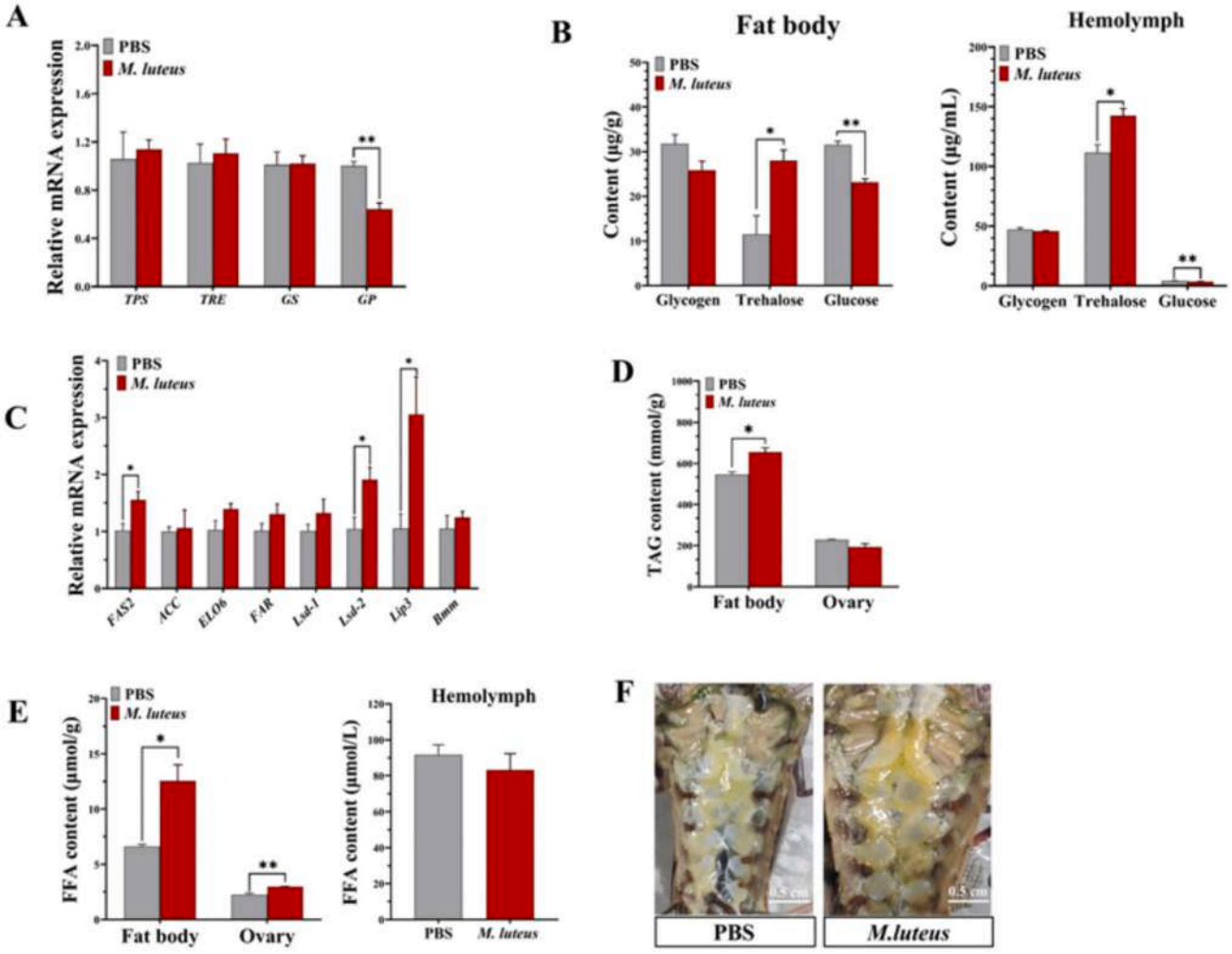

Fig. 2. Changes in energy metabolism of locusts infected with *M. luteus* were investigated. (A) Expression levels of genes associated with carbohydrate metabolic pathways were analyzed. (B) Glycogen, trehalose, and glucose contents in fat bodies and hemolymph was measured. (C) Expression levels of genes related to lipid metabolic pathways were examined. (D, E) TAG levels in fat bodies and ovaries, and FFA levels in fat bodies, ovaries, and hemolymph were measured. Each experimental group consisted of three biological replicates with a minimum of five locusts per replicate. Each value is presented as mean ± SE, and statistically significant differences between groups are denoted by * ($P < 0.05$) or ** ($P < 0.01$) using the Student's *t*-test analysis. (F) Differences in fat accumulation within the abdominal cavity of flying locusts can be visualized using a scale bar set at 0.5 cm.

than that observed in the control group (Fig. 4A). Moreover, both the quantity and weight of egg pods produced by female locusts were notably reduced compared with those in the control group. Specifically, the number of egg pods per female was approximately 1.1 in the control group, whereas it was lower in the experimental group. In addition, the number of egg grains produced by female locusts was approximately 3- and 2.6-fold higher in the control group (Figs. 4B and C). These findings indicate that infection with *M. luteus* leads to decreased fecundity in locusts.

3.5. Effects of M. luteus infection after FAS2 knockdown on immune function of locusts

The *FAS2* gene was highly expressed in the adipose bodies of locusts in previous laboratory studies, and interference with its expression resulted in the inhibition of lipid accumulation (data not shown). To further investigate the role of the *FAS2* gene during bacterial infection in locusts, its expression was suppressed through ds*FAS2* injection and its expression was assessed in the adipose body using RT-qPCR 5 d post-injection to evaluate the effectiveness of interference. Compared to the control group, ds*FAS2* injection significantly downregulated *FAS2* expression, indicating a clear interference effect (Fig. 5A). We examined changes in immune function following infestation with *M. luteus* and observed that after silencing *FAS2*, *M. luteus* infection downregulated the expression of immune pathway-related genes, including *GNBP1*, *Spaetzle*, *MyD88*, *Pelle*, and *DEF4*, and upregulated Cactus and antimicrobial peptide genes *DEF3* and *Attacin*. The expression levels of *Pelle*, *Cactus*, *DEF4*, and *Attacin* were significantly different from those in the control group (Fig. 5B). Interestingly, injection of *M. luteus* after *FAS2* knockdown notably increased lysozyme activity but had no effect on phenoloxidase levels (Fig. 5C). Furthermore, locusts with low *FAS2* expression exhibited a significantly shortened lifespan (approximately 4.0 d shorter) when injected with *M. luteus* compared to the control group (Fig. 5D). These findings suggest that silencing *FAS2* is detrimental to the survival of adult locusts.

3.6. Effects of M. luteus infection after FAS2 knockdown on energy metabolism of locusts

We used RT-qPCR to detect the expression of energy-related genes in adipose tissues and measured changes in the levels of key energy substances. Our findings indicated that *FAS2* silencing resulted in the significant downregulation of genes associated with carbohydrate metabolic pathways, including *TPS*, *TRE*, *GS*, and *GP*, during *M. luteus*

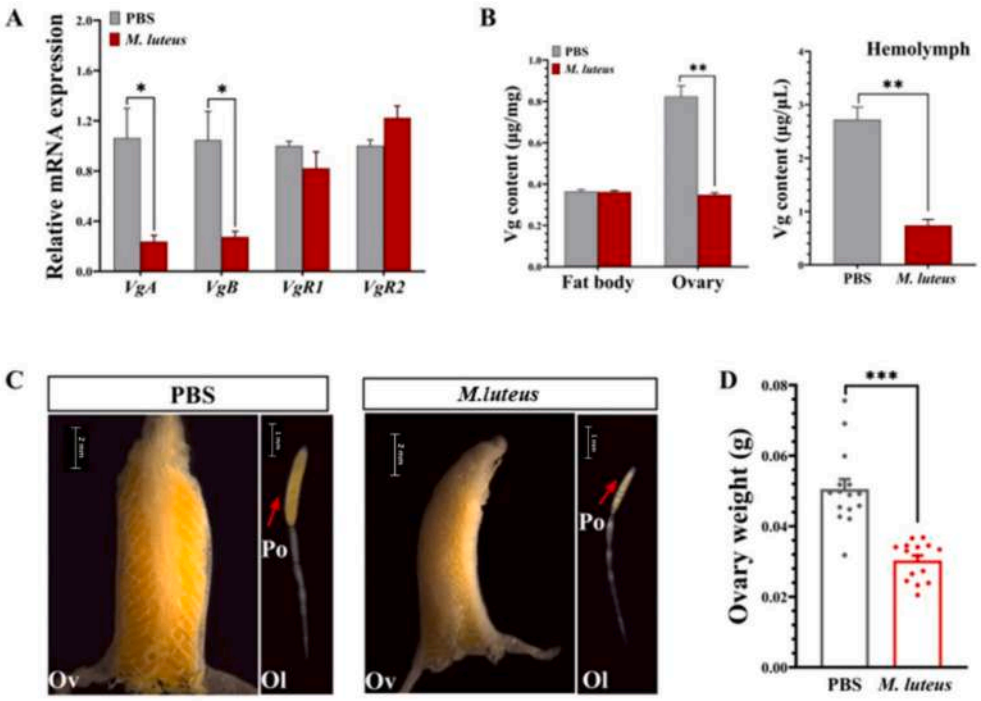

Fig. 3. Effects of *M. luteus* infection on ovarian development of locusts. (A) Expression levels of *Vgs* and *VgRs* were measured. (B) Vg protein contents in fat bodies, ovaries, and hemolymph were measured. Each group consisted of three biological replicates with a minimum of five locusts per replicate. (C) Ovarian morphology was assessed, with "Ov" representing the ovary (scale = 0.2 mm), "Ol" representing the ovarian duct, and "Po" representing the primary oocyte (scale = 0.1 mm). (D) Ovary weight was determined by dissecting at least 15 locusts per group. Each value is expressed as mean ± SE, and statistically significant differences between groups are denoted as * ($P < 0.05$), ** ($P < 0.01$), and *** ($P < 0.001$) using the Student's *t*-test.

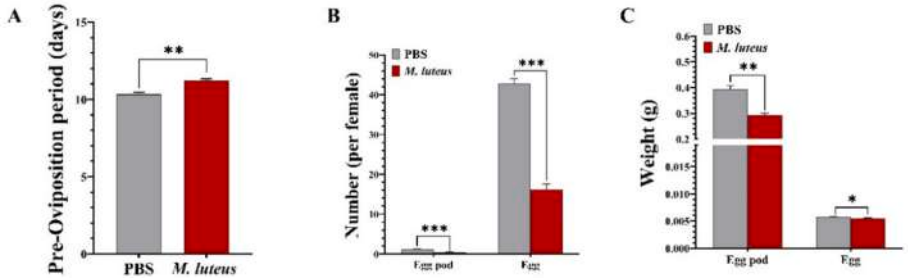

Fig. 4. Effects of *M. luteus* infection on ovulation of locusts. (A) Pre-oviposition period was assessed. (B) Changes in the number of egg pods and eggs produced by female locusts were examined. (C) Alterations in the weight of egg pods and eggs were measured. Each experimental group consisted of three biological replicates with a minimum of five locusts per replicate. Each value is expressed as mean ± SE, and statistically significant differences between groups are denoted as * ($P < 0.05$), ** ($P < 0.01$), and *** ($P < 0.001$) using the Student's t-test.

infection (Fig. 6A). Moreover, compared to the control group, *FAS2* knockdown led to reduced glycogen and glucose levels in the locust adipose tissue (Fig. 6B), and significantly increased glycogen and trehalose levels in the hemolymph (Fig. 6B). In terms of lipid metabolism, *FAS2* knockdown resulted in upregulated *Lsd-2* expression during *M. luteus* infection but significantly downregulated other genes related to lipid synthesis and catabolism (Fig. 6C). In addition, our results showed that TAG content was significantly decreased by 35.0 % and 50.5 % (after 6 d) respectively in both adipose tissue and ovaries of the experimental group compared to the control group. Moreover, the FFA content significantly decreased in the ovary but increased in the hemolymph after 6 d (Fig. 6E). Morphological observations revealed that fat accumulation within the flying locust abdominal cavities was considerably lower than that observed within the control groups following *FAS2* knockdown (Fig. 6F). These results suggest that *FAS2* is essential for lipid accumulation in locusts.

3.7. Effects of M. luteus infection after FAS2 knockdown on ovarian development and fecundity of locusts

To investigate the impact of the *FAS2* gene on locust reproduction during bacterial infection, we examined the changes in reproductive-related gene expression, vitellinogen protein content, ovarian development, and fecundity following knockdown of *FAS2* expression and injection of *M. luteus*. The results showed that silencing *FAS2* led to minimal expression of *VgA* and *VgB* in locusts infected with *M. luteus* (Fig. 7A) and reduced Vg protein content in the adipose body, ovary, and hemolymph (Fig. 7B). In addition, our study showed that *FAS2* silencing resulted in severe ovarian atrophy, dysplasia of oocytes and ovarian ducts, and a significant decrease in ovarian weight (1.7-fold) compared to the control group (Figs. 7C and D). Interestingly, locusts infected with *M. luteus* after *FAS2* knockdown exhibited significantly reduced egg-laying capacity (Fig. 7E).

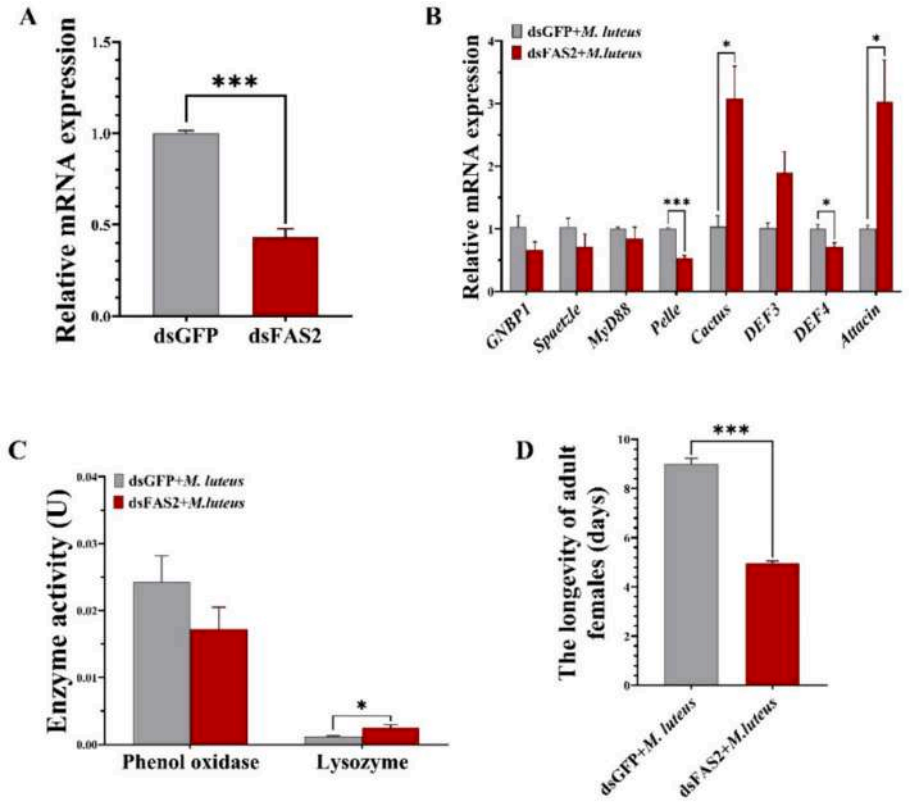

Fig. 5. Effects of *M. luteus* infection after *FAS2* knockdown on immune function of locusts. (A) Efficiency of *FAS2* silencing in adipose tissues were enhanced. (B) Expression levels of Toll immune pathway-related genes were assessed. (C) PO and lysozyme activity were evaluated. Each group consisted of three biological replicates with a minimum of five locusts per replicate. (D) Time (in days) from emergence to adult death in locusts following *M. luteus* injection was measured. Each group consisted of three biological replicates, with at least eight locusts per replicate. Each value is expressed as mean ± SE, and statistically significant differences between groups are denoted as * ($P < 0.05$), ** ($P < 0.01$), and *** ($P < 0.001$) using the Student's *t*-test.

4. Discussion

Upon pathogen invasion, the pattern recognition proteins, PGRP-SA and GNBP1, detect and bind to the pathogen, initiating an immune signal that triggers the serine protease cascade in the insect. This reaction cleaves nonactive prophenol oxidase (PPO) into active phenol oxidase (PO), leading to melanin formation and coagulation processes (Hultmark, 1993; Mavrouli et al., 2005). The extracellular cytokine, Spaetzle, subsequently undergoes activation, thereby initiating the Toll immune pathway (Hillyer, 2016). Parameters such as phenol oxidase and lysozyme activities, along with the antibacterial activity of antimicrobial peptides, are commonly used to assess the immune defense capacity of insects (González-Santoyo and Córdoba-Aguilar, 2012; Hu et al., 2022). Insect defensin is a cysteine-rich antimicrobial peptide that exhibits potent activity against Gram-positive bacteria. Attacin primarily targets gram-negative bacteria but has also demonstrated efficacy against certain gram-positive bacteria in specific insects (Bang et al., 2012; Yi et al., 2014). Injection of *M. luteus* strongly induced *DEF3* and *Attacin* gene expression, which encode antimicrobial peptides, highlighting their crucial role in combating *M. luteus* infections (Fig. 1A). However, silencing *FAS2* during bacterial infection reduces the expression levels of several immune-related genes. Although *DEF3* and *Attacin* exhibited upregulation patterns similar to those observed in the control group, the extent of upregulation was comparatively lower (Fig. 5B). Phenoloxidase and lysozyme play crucial roles in humoral immunity in insects, as demonstrated in Diptera (Hillyer and Christensen, 2005; Bruno et al., 2021), Lepidoptera (Jiang et al., 2010; Radwan et al., 2022), Orthoptera (da Silva et al., 2000; Adamo et al., 2016), and other insect species. This study revealed that locusts can resist *M. luteus* infection by enhancing phenoloxidase activity (Fig. 1B). Such selective activation of specific immune responses may represent an adaptive strategy used by insects to minimize the costs associated with immune defense mechanisms (Moret, 2003). Interestingly, silencing *FAS2* resulted in an opposite pattern of changes in phenol oxidase and lysozyme activities compared to stimulation with bacteria alone. Dual pressure led to a decrease in phenol oxidase activity, but an increase in lysozyme activity (Fig. 5C). This can be attributed to the high energy expenditure associated with activating and maintaining the PO cascade (González-Santoyo and Córdoba-Aguilar, 2012). Immune attacks affect the energy metabolism of locusts (Fig. 2) and, as was confirmed by our findings (Fig. 1C and D), this compound effect poses a threat to insect survival. Moreover, this detrimental effect was exacerbated by the reduced *FAS2* expression (Fig. 5D). Further studies may consider using sublethal concentrations to achieve a more optimal treatment effect.

A robust immune response during immune challenges necessitates precise and timely allocation of energy to appropriate cells or tissues for efficient self-defense mechanisms (Dolezal et al., 2019; Moret, 2003). Immunity is a fundamental physiological process crucial for survival and has been reported to provide preferential access to energy resources (Dolezal et al., 2019). This phenomenon was evident in our study, where we observed significantly elevated levels of TAG and FFA in the fat bodies of locusts during bacterial infection, accompanied by decreased TAG levels in the ovary. This strategic nutrient allocation may enhance the functionality of the immune system by accumulating lipids in the fat body (Figs. 2D and E). However, the glucose content in the fat body was significantly reduced, suggesting that sugar serves as the primary energy source used by locusts when confronted with immune stimulation alone (Figs. 2B, D, and E). Previous studies have shown that glucose represents a significant energy expenditure for insects during immune challenges, and that immune system activation leads to varying degrees of glucose

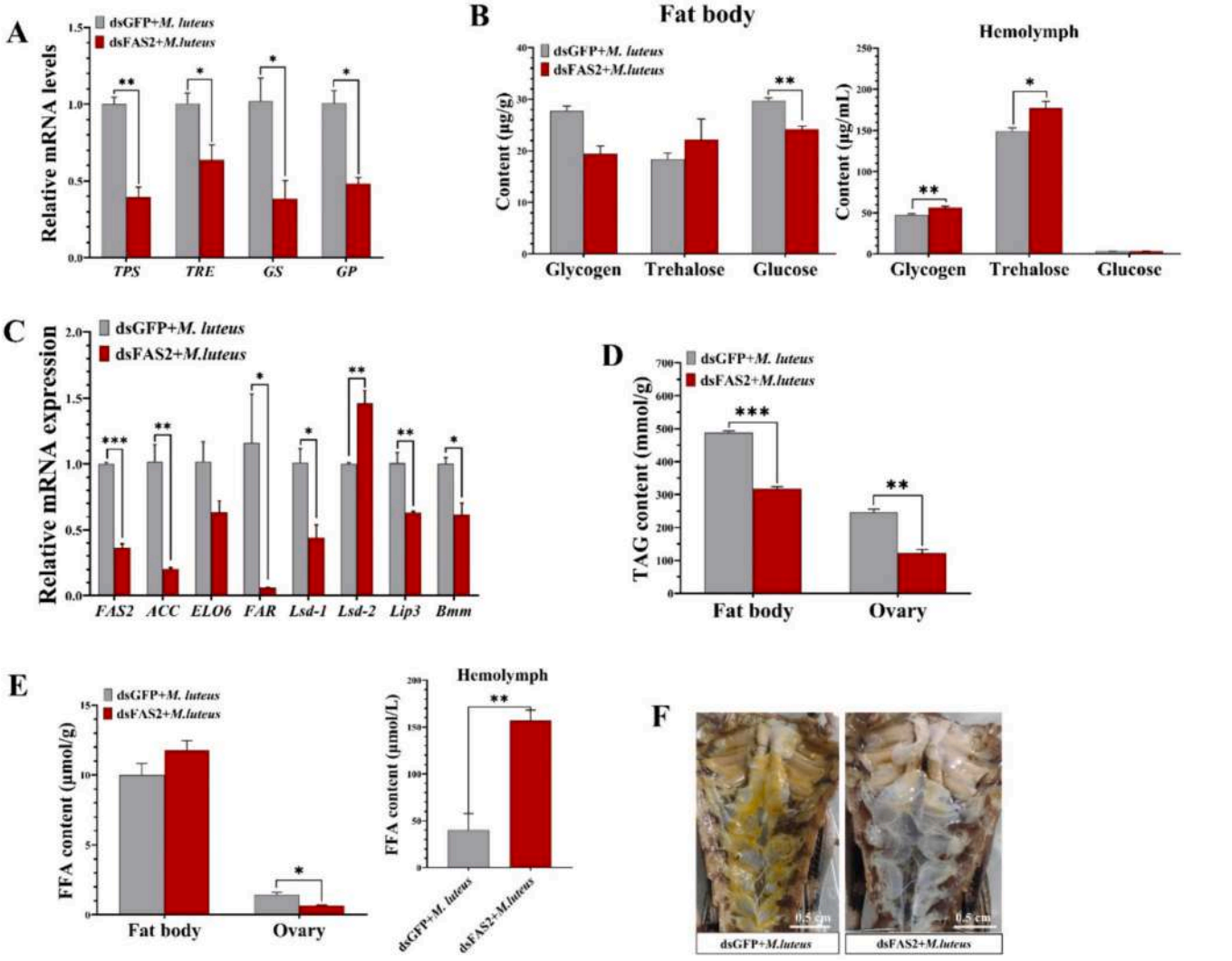

Fig. 6. Effects of *M. luteus* infection after *FAS2* knockdown on carbohydrate and lipid metabolism of locusts. (A) Expression levels of genes associated with carbohydrate metabolic pathways were measured. (B) Glycogen, trehalose, and glucose contents in fat bodies and hemolymph were measured. (C) Expression levels of genes involved in lipid metabolic pathways were assessed. (D, E) TAG levels in fat bodies and ovaries, and FFA levels in fat bodies, ovaries, and hemolymph were measured. Each experimental group consisted of three biological replicates with a minimum of five locusts per replicate. Each value is expressed as mean ± SE, and statistically significant differences between groups are denoted as * ($P < 0.05$), ** ($P < 0.01$), and *** ($P < 0.001$) using the Student's *t*-test. (F) Fat accumulation in the abdominal cavities of flying locusts was visualized (scale = 0.2 mm).

reduction (Dolezal et al., 2019). Following *FAS2* silencing, the expression of pivotal genes involved in lipid and carbohydrate synthesis and breakdown pathways was nearly abolished, resulting in a substantial depletion of the adipose body reserves of lipids and glycogen (Fig. 6). Upon bacterial infection following *FAS2* silencing, locusts initiate the mobilization of both lipid and glycogen breakdown processes as a reflection of their heightened energy demand for self-protection against dual stressors. This resulted in diminished energy availability (Figs. 6B, D, and E). In a related study by Pompka et al. (2022), fifth instar larvae of *Spodoptera exigua* exhibited reduced glycogen concentrations under the combined stress conditions of starvation and cadmium exposure.

Because of the high energy demands of immunity and reproduction, competition for energy resources may exist between these two functions. Pathogen infections have a negative effect on fecundity (Howick and Lazzaro, 2014; Schwenke et al., 2016; Nystrand and Dowling, 2020; Breiner et al., 2022). In orthopterans, activation of the immune response has also been associated with reduced egg production (Bascuñán-García et al., 2010). However, the mechanisms underlying the trade-off between insect immunity and reproduction remain poorly understood. Our study revealed that when exposed to bacterial infection alone, the Vg synthesis volume decreased significantly. *M. luteus* infection resulted in impaired oocyte and ovary development, reduced egg quantity and quality, and a significantly prolonged pre-egg stage in the locusts (Figs. 3 and 4). Transcription of *Vg* genes in adipose tissues is severely inhibited, leading to decreased Vg protein content in hemolymph circulation and oocyte deposition, which is likely the primary cause of reduced fecundity. However, when faced with both low *FAS2* expression and bacterial infection, fertility damage in locusts is exacerbated. At the microscopic level, this double pressure further suppressed *Vg* expression in fat bodies, resulting in decreased Vg protein content within fat bodies, hemolymph circulation, and ovaries (Figs. 7A and B). On a macroscopic scale, this dual stress caused significant delays in ovarian development, rendering females unable to lay eggs, evident by the thinning of ovarian ducts even up to day 8 post-emergence (Figs. 7C and D). Lipid and Vg synthesis is obstructed, leading to the inadequate uptake of Vg, lipids, and other nutrients by the oocytes, which directly compromises female fertility.

In summary, the infection of *M. luteus* triggers the activation of the immune system in locusts. The host organism responds by synthesizing a substantial amount of antimicrobial peptides, phenol oxidases, and

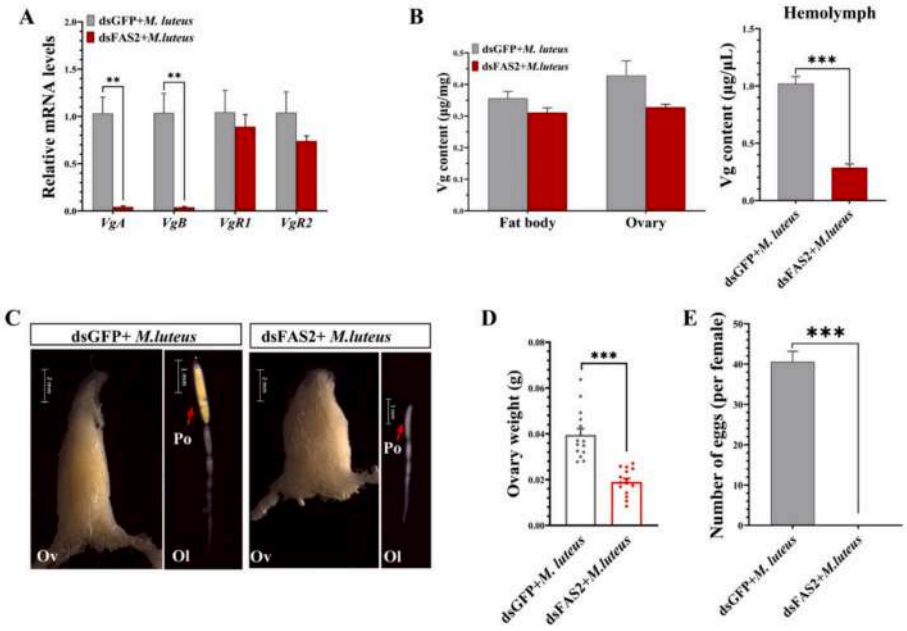

Fig. 7. Effects of *M. luteus* infection after *FAS2* knockdown on ovarian development and fecundity of locusts. (A) Expression levels of *Vgs* and *VgRs* were measured. (B) Vg protein contents in fat bodies, ovaries, and hemolymph were measured. Each group consisted of three biological replicates with a minimum of five locusts per replicate. (C) Ovarian morphology was examined, with ovaries (scale = 0.2 mm), ovarian ducts, and primary oocytes (scale = 0.1 mm) represented by Ov, Ol, and Po, respectively. (D) Ovarian weight was determined for each group using at least 15 dissected locusts. Each value is expressed as mean ± SE, and statistically significant differences between groups are denoted as * ($P < 0.05$), ** ($P < 0.01$), and *** ($P < 0.001$) using the Student's t-test.

other immune factors to combat infection. In addition, it regulates lipid and glucose metabolism to maintain the energy balance. However, the immune response competes for energy resources that are otherwise used for reproduction, thereby resulting in reduced fertility. This effect is further exacerbated when *FAS2* function is impaired along with *M. luteus* attack, leading to a more severe depletion of energy reserves. Despite activation of the immune system under low-energy conditions, there appears to be a decrease in the overall immune capacity, as adults can only survive for a short period under these dual pressures. Moreover, their ability to lay eggs is significantly compromised by the prioritization of energy allocation toward immunity. The aforementioned findings are valuable for investigating the molecular mechanisms underlying the trade-off between immunity and reproduction in locusts, and thus have significant implications for the population density control of these insects.

CRediT authorship contribution statement

Tingting Ma: Writing – original draft, Validation, Investigation, Data curation. **Ya Tang:** Writing – original draft, Investigation, Data curation. **Yi Jin:** Investigation. **Jiaying Xu:** Supervision. **Huazhang Zhao:** Conceptualization. **Min Zhou:** Data curation. **Bin Tang:** Project administration. **Shigui Wang:** Writing – review & editing, Methodology, Investigation, Formal analysis.

Declaration of competing interest

The authors declare no competing interest.

Data availability

Data will be made available on request.

Acknowledgments

This research was supported by the National Natural Science Foundation of China (Grant Nos. 30970473 and 31270459), and the Qianjiang Talents Fund of Zhejiang Province (2010R10093), and National College Students Innovation and Entrepreneurship Training Program (Grant Number 202410346019).

References

Adamo, S.A., Davies, G., Easy, R., Kovalko, I., Turnbull, K.F., 2016. Reconfiguration of the immune system network during food limitation in the caterpillar *Manduca sexta*. J. Exp. Biol. 219 (Pt 5), 706–718.

Alabaster, A., Isoe, J., Zhou, G., Lee, A., Murphy, A., Day, W.A., Miesfeld, R.L., 2011. Deficiencies in acetyl-CoA carboxylase and fatty acid synthase 1 differentially affect eggshell formation and blood meal digestion in *Aedes aegypti*. Insect Biochem. Mol. Biol. 41 (12), 946–955.

Arrese, E.L., Soulages, J.L., 2010. Insect fat body: energy, metabolism, and regulation. Annu. Rev. Entomol. 55, 207–225.

Bang, K., Park, S., Yoo, J.Y., Cho, S., 2012. Characterization and expression of attacin, an antibacterial protein-encoding gene, from the beet armyworm, *Spodoptera exigua* (Hübner) (Insecta: Lepidoptera: Noctuidae). Mol. Biol. Rep. 39 (5), 5151–5159.

Bascuñán-García, A.P., Lara, C., Córdoba-Aguilar, A., 2010. Immune investment impairs growth, female reproduction and survival in the house cricket, *Acheta domesticus*. J. Insect Physiol. 56 (2), 204–211.

Breiner, D.J., Whalen, M.R., Worthington, A.M., 2022. The developmental high wire: balancing resource investment in immunity and reproduction. Ecol. Evol. 12 (4), e8774.

Bruno, D., Montali, A., Mastore, M., Brivio, M.F., Mohamed, A., Tian, L., Grimaldi, A., Casartelli, M., Tettamanti, G., 2021. Insights into the immune response of the black soldier fly larvae to bacteria. Front. Immunol. 12, 745160.

Canavoso, L.E., Jouni, Z.E., Karnas, K.J., Pennington, J.E., Wells, M.A., 2001. Fat metabolism in insects. Annu. Rev. Nutr. 21, 23–46.

Cerenius, L., Lee, B.L., Söderhäll, K., 2008. The proPO-system: pros and cons for its role in invertebrate immunity. Trends Immunol. 29 (6), 263–271.

Cong, L., Yang, W., Jiang, X., Niu, J., Shen, G., Ran, C., Wang, J., 2015. The essential role of Vitellogenin receptor in ovary development and Vitellogenin uptake in *Bactrocera dorsalis* (Hendel). Int. J. Mol. Sci. 16, 18368–18383.

da Silva, C.C., Dunphy, G.B., Rau, M.E., 2000. Interaction of *Xenorhabdus nematophilus* (Enterobacteriaceae) with the antimicrobial defenses of the house cricket, *Acheta domesticus*. J. Invertebr. Pathol. 76, 285–292.

Denno, R.F., 1994. Life history variation in Planthoppers. In: In: Planthoppers: Their Ecology and Management. Springer US, Boston, MA, pp. 163–215.

Dolezal, T., Krejcova, G., Bajgar, A., Nedbalova, P., Strasser, P., 2019. Molecular regulations of metabolism during immune response in insects. Insect Biochem. Mol. Biol. 109, 31–42.

Friedman, S., 1978. Treholose regulation, one aspect of metabolic homeostasis. Annu. Rev. Entomol. 23 (1), 389–407.

González-Santoyo, I., Córdoba-Aguilar, A., 2012. Phenoloxidase: a key component of the insect immune system. Entomol. Exp. Appl. 142, 1–16.
Guo, J., Dong, S., Ye, G., Li, K., Zhu, J., Fang, Q., Hu, C., 2011. Oosorption in the endoparasitoid, *Pteromalus puparum*. J. Insect Sci. 11, 90.
Gupta, V., Frank, A.M., Matolka, N., Lazzaro, B.P., 2022. Inherent constraints on a polyfunctional tissue lead to a reproduction-immunity tradeoff. BMC Biol. 20 (1), 127.
Han, S., Wang, D., Song, P., Zhang, S., He, Y., 2022. Molecular characterization of Vitellogenin and its receptor in Spodoptera frugiperda (J. E. Smith, 1797), and their function in reproduction of female. Int. J. Mol. Sci. 23 (19), 11972.
Heier, C., Kühnlein, R.P., 2018. Triacylglycerol metabolism in *Drosophila melanogaster*. Genetics 210 (4), 1163–1184.
Hillyer, J.F., 2016. Insect immunology and hematopoiesis. Dev. Comp. Immunol. 58, 102–118.
Hillyer, J.F., Christensen, B.M., 2005. Mosquito phenoloxidase and defensin colocalize in melanization innate immune responses. J. Histochem. Cytochem. 53 (6), 689–698.
Hou, Y., Wang, X., Saha, T.T., Roy, S., Zhao, B., Raikhel, A.S., Zou, Z., 2015. Temporal coordination of carbohydrate metabolism during mosquito reproduction. PLoS Genet. 11 (7), e1005309.
Hough, J., Howard, J.D., Brown, S., Portwood, D.E., Kilby, P.M., Dickman, M.J., 2022. Strategies for the production of dsRNA biocontrols as alternatives to chemical pesticides. Front. Bioeng. Biotechnol. 10, 980592.
Howick, V.M., Lazzaro, B.P., 2014. Genotype and diet shape resistance and tolerance across distinct phases of bacterial infection. BMC Evol. Biol. 14 (1), 56.
Hu, Y., Wang, S., Tang, Y., Xie, G., Ding, Y., Xu, Q., Tang, B., Zhang, L., Wang, S., 2022. Suppression of yolk formation, oviposition and egg quality of locust (*Locusta migratoria manilensis*) infected by *Paranosema locustae*. Front. Immunol. 13, 848267.
Hultmark, D., 1993. Immune reactions in Drosophila and other insects: a model for innate immunity. Trends Genet. 9 (5), 178–183.
Jehan, C., Sabarly, C., Rigaud, T., Moret, Y., 2022. Senescence of the immune defences and reproductive trade-offs in females of the mealworm beetle, *Tenebrio molitor*. Sci. Rep. 12 (1), 19747.
Jiang, H., Vilcinskas, A., Kanost, M.R., 2010. Immunity in lepidopteran insects. Adv. Exp. Med. Biol. 708, 181–204.
Kawooya, J.K., Law, J.H., 1988. Role of lipophorin in lipid transport to the insect egg. J. Biol. Chem. 263 (18), 8748–8753.
King, B., Li, S., Liu, C., Kim, S.J., Sim, C., 2020. Suppression of glycogen synthase expression reduces glycogen and lipid storage during mosquito overwintering diapause. J. Insect Physiol. 120, 103971.
Levitin, A., Whiteway, M., 2008. *Drosophila* innate immunity and response to fungal infections. Cell. Microbiol. 10 (5), 1021–1026.
Li, L., Jiang, Y., Liu, Z., You, L., Wu, Y., Xu, B., Ge, L., Stanley, D., Song, Q., Wu, J., 2016. Jinggangmycin increases fecundity of the brown planthopper, *Nilaparvata lugens* (Stål) via fatty acid synthase gene expression. J. Proteome 130, 140–149.
Lourenco, A.P., Martins, J.R., Bitondi, M.M., Simões, Z.L., 2009. Trade-off between immune stimulation and expression of storage protein genes. Arch. Insect Biochem. Physiol. 71 (2), 70–87.
Ma, L., Zhang, W., Liu, C., Chen, L., Xu, Y., Xiao, H., Liang, G., 2018. Methoprene-tolerant (met) is indispensable for larval metamorphosis and female reproduction in the cotton bollworm *Helicoverpa armigera*. Front. Physiol. 9, 1601.
Mavrouli, M.D., Tsakas, S., Theodorou, G.L., Lampropoulou, M., Marmaras, V.J., 2005. MAP kinases mediate phagocytosis and melanization via prophenoloxidase activation in medfly hemocytes. Biochim. Biophys. Acta 1744 (2), 145–156.
Mollaei, M., Izadi, H., Moharramipour, S., Behroozi Moghadam, E., 2017. Physiology of hibernating larvae of the pistachio twig borer, *Kermania pistaciella* Amsel (Lepidoptera: Tineidae), collected from Akbari cultivar of *Pistacia vera L.* Neotrop. Entomol. 46 (1), 58–65.
Moret, Y., 2003. Explaining variable costs of the immune response: selection for specific versus non-specific immunity and facultative life history change. Oikos 102, 213–216.
Moriconi, D.E., Dulbecco, A.B., Juárez, M.P., Calderón-Fernández, G.M., 2019. A fatty acid synthase gene (FASN3) from the integument tissue of *Rhodnius prolixus* contributes to cuticle water loss regulation. Insect Mol. Biol. 28 (6), 850–861.
Nystrand, M., Dowling, D.K., 2020. Effects of immune challenge on expression of life-history and immune trait expression in sexually reproducing metazoans-a meta-analysis. BMC Biol. 18 (1), 135.
Pei, X., Chen, N., Bai, Y., Qiao, J., Li, S., Fan, Y., Liu, T., 2019. *BgFas1*: a fatty acid synthase gene required for both hydrocarbon and cuticular fatty acid biosynthesis in the German cockroach, *Blattella germanica* (L.). Insect Biochem. Mol. Biol. 112, 103203.
Pompka, A., Szulińska, E., Kafel, A., 2022. Starvation and cadmium affect energy reserves and oxidative stress in individuals of *Spodoptera exigua*. Ecotoxicology 31 (9), 1346–1355.
Radwan, M.H., Alaidaroos, B.A., Jastaniah, S.D., Abu El-Naga, M.N., El-Gohary, E.E., Barakat, E.M.S., ElShafie, A.M., Abdou, M.A., Mostafa, N.G., El-Saadony, M.T., Momen, S.A.A., 2022. Evaluation of antibacterial activity induced by *Staphylococcus aureus* and Ent a in the hemolymph of *Spodoptera littoralis*. Saudi. J. Biol. Sci. 29 (4), 2892–2903.
Roth, T.F., Porter, K.R., 1964. Yolk protein uptake in the oocyte of the mosquito *Aedes Aegypti*. L. J. Cell Biol. 20 (2), 313–332.
Sangbaramou, R., Camara, I., Huang, X., Shen, J., Tan, S., Shi, W., 2018. Behavioral thermoregulation in *Locusta migratoria manilensis* (Orthoptera: Acrididae) in response to the entomopathogenic fungus, *Beauveria bassiana*. PLoS One 13 (11), 0206816.
Schwenke, R.A., Lazzaro, B.P., Wolfner, M.F., 2016. Reproduction-immunity trade-offs in insects. Annu. Rev. Entomol. 61, 239–256.
Shukla, E., Thorat, L.J., Nath, B.B., Gaikwad, S.M., 2015. Insect trehalase: physiological significance and potential applications. Glycobiology 25 (4), 357–367.
Sugahara, R., Tanaka, S., Jouraku, A., Shiotsuki, T., 2017. Geographic variation in RNAi sensitivity in the migratory locust. Gene 605, 5–11.
Tan, Q., Liu, W., Zhu, F., Lei, C., Wang, X., 2017. Fatty acid synthase 2 contributes to diapause preparation in a beetle by regulating lipid accumulation and stress tolerance genes expression. Sci. Rep. 7, 40509.
Tang, Y., Hu, Y., Wang, S., Zhou, M., Ding, Y., Cai, S., Tang, B., Wang, S., 2023. RNAi-mediated CrebA silencing inhibits reproduction and immunity in *Locusta migratoria manilensis*. Dev. Comp. Immunol. 145, 104711.
Telfer, W.H., 1954. Immunological studies of insect metamorphosis. II. The role of a sex-limited blood protein in egg formation by the Cecropia silkworm. J. Gen. Physiol. 37 (4), 539–558.
Toprak, U., Hegedus, D., Doğan, C., Güney, G., 2020. A journey into the world of insect lipid metabolism. Arch. Insect Biochem. Physiol. 104 (2), e21682.
Visser, B., Ellers, J., 2008. Lack of lipogenesis in parasitoids: a review of physiological mechanisms and evolutionary implications. J. Insect Physiol. 54 (9), 1315–1322.
Wang, S., Li, G.Y., Liu, Y., Luo, Y., Xu, C., Li, C., Tang, B., 2020a. Regulation of carbohydrate metabolism by Trehalose-6-phosphate synthase 3 in the Brown Planthopper, *Nilaparvata lugens*. Front. Physiol. 11, 575485.
Wang, J., Shen, L., Xing, X., Xie, Y., Li, Y., Liu, Z., Wang, J., Wu, F., Sheng, S., 2020b. Lipid dynamics, identification, and expression patterns of fatty acid synthase genes in an Endoparasitoid, *Meteorus pulchricornis* (Hymenoptera: Braconidae). Int. J. Mol. Sci. 21 (17), 6228.
Wu, Z., Yang, L., He, Q., Zhou, S., 2021. Regulatory mechanisms of Vitellogenesis in insects. Front. Cell Dev. Biol. 8, 593613.
Yi, H., Chowdhury, M., Huang, Y., Yu, X., 2014. Insect antimicrobial peptides and their applications. Appl. Microbiol. Biotechnol. 98 (13), 5807–5822.
Zeng, B., Kang, K., Wang, H., Pan, B., Xu, C., Tang, B., Zhang, D., 2020. Effect of glycogen synthase and glycogen phosphorylase knockdown on the expression of glycogen- and insulin-related genes in the rice brown planthopper *Nilaparvata lugens*. Comp. Biochem. Physiol. Part D Genom. Proteom. 33, 100652.
Zhang, W., Tettamanti, G., Bassal, T., Heryanto, C., Eleftherianos, I., Mohamed, A., 2021. Regulators and signalling in insect antimicrobial innate immunity: functional molecules and cellular pathways. Cell. Signal. 83, 110003.